Research Square

Preprints are preliminary reports that have not undergone peer review.
They should not be considered conclusive, used to inform clinical practice,
or referenced by the media as validated information.

Negative-polarity-selective non-contact breakup of oppositely charged droplets

Zhishan Wang
Jiangsu University
Yuanping Huo
huoyuanping@ujs.edu.cn
Jiangsu University
Zhuohang Li
Jiangsu University
Zirui Wang
Jiangsu University
Zhentao Wang
Jiangsu University
Huihe Qiu
Hong Kong University of Science and Technology
Junfeng Wang
Chongqing University

Research Article

Keywords: Oppositely charged droplets, Non-contact breakup, Gas ionization, Space charge, Coulomb fission, Electrohydrodynamics

Posted Date: June 19th, 2026

DOI: https://doi.org/10.21203/rs.3.rs-9966560/v1

License: This work is licensed under a Creative Commons Attribution 4.0 International License.
Read Full License

Additional Declarations: No competing interests reported.

Version of Record: A version of this preprint was published at Experiments in Fluids on September 30th, 2026. See the published version at https://doi.org/10.1007/s00348-026-04327-7.

Negative-polarity-selective non-contact breakup of oppositely charged droplets

Zhishan Wang[1], Yuanping Huo[1]*, Zhuohang Li[1], Zirui Wang[1], Zhentao Wang[1], Huihe Qiu[2], Junfeng Wang[3]

AFFILIATIONS

[1]School of Energy and Power Engineering, Jiangsu University, Zhenjiang, Jiangsu 212013, China
[2]Department of Mechanical and Aerospace Engineering, Hong Kong University of Science and Technology, Hong Kong, China
[3]School of Energy and Power Engineering, Chongqing University, Chongqing, 400000, China

*Corresponding author: Yuanping Huo, huoyuanping@ujs.edu.cn

Abstract

The non-contact interaction of oppositely charged droplets under strong electric fields involves coupled charge transport, gas ionization and interfacial instability, yet direct evidence for the origin of polarity-selective breakup remains limited. Here, non-contact breakup of highly conducting oppositely charged droplets was investigated in air and helium using a self-developed microscopic collision platform and high-speed imaging. By varying droplet curvature, reversing the high-voltage-electrode polarity and comparing acidic and alkaline electrolytes, we show that breakup in air consistently initiates from the negative-polarity droplet. The polarity preference is therefore not governed by droplet geometry, electrode configuration or liquid-phase ion mobility. In helium, the breakup at the negative side becomes weaker and, in some cases, non-contact breakup occurs at both polarity sides. For a given liquid conductivity, the critical

voltage for breakup is also higher in helium than in air. We attribute this behavior to impact ionization in air: slowly migrating positive ions accumulate near the negatively charged droplet, distort the local electric field and increase the surface charge density until a local sub-Rayleigh instability is reached. In helium, weak electron attachment and faster charged-particle transport reduce this field asymmetry. These results demonstrate that gas ionization regulates breakup polarity and the dynamic outcome of oppositely charged droplets, providing guidance for electrosprays, microreactors and electric-field-controlled multiphase flows.

Keywords: Oppositely charged droplets; Non-contact breakup; Gas ionization; Space charge; Coulomb fission; Electrohydrodynamics

1 Introduction

The interaction between oppositely charged droplets is a fundamental problem in electrohydrodynamics and is encountered in a wide range of processes, including electrosprays, microreactors, fuel atomization, particle capture, and electric-field-assisted control of multiphase flows (Zhou et al. 2024; Giusti and Fredrich 2024; Liu et al. 2024; Xu et al. 2025; Wang et al. 2020). When two droplets carrying opposite charges approach each other, their interfaces may undergo coalescence, rebound, non-coalescence, or breakup, depending on the competition among electric stresses, capillary forces, and fluid motion. Clarifying the mechanisms that govern these dynamic outcomes is therefore important for understanding and controlling charged-droplet systems.

Since Rayleigh (1882) proposed the critical breakup criterion for charged droplets, the understanding of the stability of charged droplets has continued to advance. The evolution of collision modes between charged droplets is essentially an external manifestation of electrohydrodynamic effects, with the underlying mechanism governed by the coupling of electric forces, hydrodynamic forces, and surface tension. Early studies mainly focused on coalescence and rebound following droplet contact. Ristenpart et al. (2009) experimentally demonstrated that oppositely charged droplets do not always coalesce after contact; instead, a coalescence–rebound transition controlled by the electric Bond number exists. They further proposed a criterion based on the critical tip angle of the droplets. Subsequently, Hamlin et al. (2012) reported partial coalescence under low-conductivity conditions, while Liu et al. (2012) observed non-coalescence behavior in pH-sensitive emulsions. Liu et al. (2021) analyzed the collision and coalescence behavior of micro- and nanometer-sized droplets under an applied electric field and showed that droplet charge and electric field strength can significantly alter collision modes and shorten the coalescence time. Sun et al. (2024) investigated the cooperative coalescence of multiple-droplet systems under a constant direct-current electric field and found that the electric field can effectively promote collisions and coalescence among multiple droplets. In addition, Plog et al. (2021) investigated the coalescence of sessile droplets driven by an electric field in a jetting-based printing framework and showed that droplets initially separated with little chance of natural coalescence could be forced to merge by the applied field. These studies have

provided important insight into charged-droplet dynamics, but they mainly concern low-conductivity liquids or processes that occur after physical contact.

When the droplet conductivity is high or the applied electric field is strong, the interfacial response becomes more complex. Shrimpton (2005) pointed out that local Coulomb fission may occur even when the total charge of a droplet remains below the Rayleigh limit, indicating that local charge accumulation can dominate the onset of interfacial instability. Wang et al. (2014) observed a clear polarity preference during the breakup of oppositely charged conducting droplets, where breakup occurred preferentially on the side connected to the negative high-voltage electrode. This behavior was referred to as negative-polarity contact breakup. Bhalwankar et al. (2023) subsequently studied binary collisions of water drops in a horizontal electric field and found that the applied field enhances electrohydrodynamic effects and promotes breakup on the negative-polarity side. Pawar et al. (2024) further showed that the combined effects of collision eccentricity and a horizontal electric field can alter the collision outcome, with the end facing the negative electrode becoming more susceptible to instability as the field strength increases. Huo et al. (2020) showed that the competition between gas ionization and the attainment of the local Rayleigh limit can determine non-contact rebound and breakup between adjacent oppositely charged droplets, suggesting that the surrounding gas is not merely a passive medium. In addition, Meng et al. (2025) recently reported that approaching oppositely charged microdroplets can spontaneously generate microdischarges and ionize the surrounding

gas, further indicating that gas-phase processes may participate in droplet interfacial instability.

Despite these advances, systematic studies on the breakup behavior of highly conductive droplets under non-contact conditions and the mechanism underlying polarity selection are still lacking. Direct comparative experimental evidence is still lacking as to whether and how gas ionization determines the polarity selection of non-contact breakup in oppositely charged droplets. To address this issue, we investigate the non-contact interaction of oppositely charged droplets under strong electric fields using a high-speed microscopic observation platform operated in air and helium environments. The use of helium provides an effective way to modify gas ionization and charged-particle transport in the inter-droplet gap. By varying the droplet interfacial curvature, reversing the polarity of the high-voltage electrode, and comparing acidic and alkaline electrolyte solutions, we first examine whether negative-polarity breakup originates from droplet geometry, electrode configuration, or liquid-phase ion migration. We then compare the interfacial evolution in air and helium to analyze the breakup location, breakup intensity, and critical voltage for non-contact breakup. This study provides experimental evidence and mechanistic insight into non-coalescent interactions between charged droplets and interfacial instability in electric-field-controlled multiphase flows.

2 Experimental Setup and Theoretical Model

2.1 Experimental Setup

Fig. 1 shows the experimental setup used to investigate the non-contact interaction between oppositely charged droplets. The system mainly consists of a high-voltage power supply, a micrometer translation stage, a droplet generation and support unit, a gas-controlled chamber, and a high-speed microscopic imaging system. The lower droplet was placed on a homemade hydrophobic substrate, while the upper droplet was suspended from the end of a copper wire. During the experiments, the two droplets were aligned along the vertical direction to maintain geometric symmetry as they approached each other (Lee et al. 2012). Droplets of comparable size were generated at the upper and lower electrodes using a microsyringe. One terminal of the high-voltage power supply was connected either to the upper copper wire or to the lower substrate, while the other terminal was grounded, so that the two droplets carried opposite charges. The upper droplet was then driven slowly toward the lower droplet by the micrometer translation stage at a speed of approximately 0.03 mm/s. This quasi-static approach helped to reduce inertial effects, allowing the experiments to focus on electric-field-induced interfacial deformation, gas ionization, and non-contact breakup. The droplet interaction process was recorded using an Olympus i-SPEED 3 high-speed camera equipped with a NAVITAR 12× microscopic zoom lens. The frame rate was 15,000 fps, and the image resolution was 432×320 pixels. Back illumination was provided by a 40 W high-intensity LED cold light source placed opposite the camera to obtain a clear outline of the gas–liquid interface. Before the experiments, the focal distance and magnification were calibrated, and the relevant components were grounded to reduce the influence of electrostatic accumulation. Experiments were conducted in both air and

helium environments. The helium environment was obtained by continuously supplying helium into a transparent plexiglass enclosure, which was used to modify the gas ionization and charged-particle transport characteristics in the inter-droplet gap. The ambient temperature was maintained at 25±0.5 ºC, and the relative humidity was approximately 30%. The test liquids included deionized water, a 20 wt.% hydrochloric acid solution, and a 20 wt.% sodium hydroxide solution. Their electrical conductivities were measured using a Hana HI993310 conductivity meter, and the corresponding values are listed in Table 1.

This study focuses on the polarity selection of non-contact breakup in oppositely charged droplets. By varying the high-voltage electrode polarity, droplet interfacial curvature, solution pH, and surrounding gas environment, we systematically examine whether non-contact breakup always occurs on the negative-polarity side and further analyze its relationship with gas ionization.

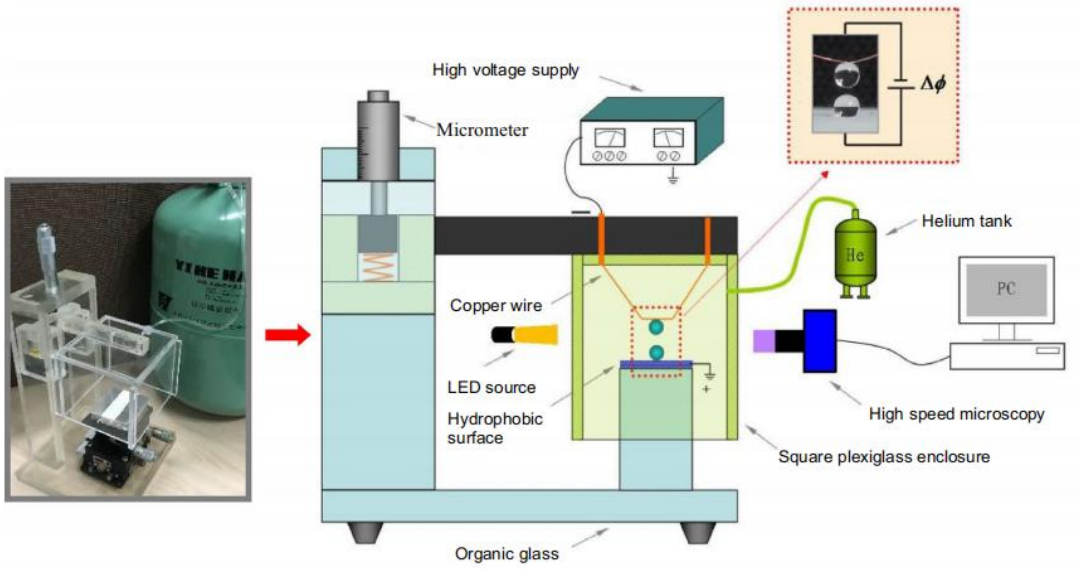

Fig. 1 Experimental setup for non-contact interactions between oppositely charged droplets in a gas-controlled chamber

Table 1 Properties of the working liquids used in the experiments

Experimental Medium	Mass Fraction (wt.%)	Conductivity (μS/cm)
HCl Aqueous Solution	20	820
NaOH Aqueous Solution	20	414

2.2 Charge Distribution and Interfacial Instability of Charged Droplets

The interfacial evolution of charged droplets subjected to an external electric field is fundamentally determined by the competition among the surface charge distribution and the various forces induced by it. In theory, the surface charge density of a droplet is uniformly distributed. The stability of the droplet is governed by the balance between the hydrostatic pressure difference, P_s, and the expansion force, P_e , which arise from surface tension and Coulomb repulsion, respectively, as illustrated in Fig. 2.

$$P_S = \frac{2\gamma}{R} \tag{1}$$

$$P_e = \frac{1}{2}\varepsilon_0 E_n^{\,2} \tag{2}$$

Where γ is the surface tension, R is the droplet radius, ε_0 is the vacuum permittivity, and E_n is the normal component of the interfacial electric field. When $P_e = P_s$, the droplet reaches its stability limit, known as the Rayleigh limit (Rayleigh 1882; Pelesz and Zylka 2020), corresponding to the critical charge:

$$Q = 8\pi\sqrt{\varepsilon\sigma}r^{2/3} \tag{3}$$

At this point, the surface energy and electrostatic energy are in equilibrium. When the expansion force P_e on the droplet exceeds the capillary pressure difference P_s, this balance is disrupted, and the droplet tip becomes unstable, forming a Taylor cone (Taylor 1964).

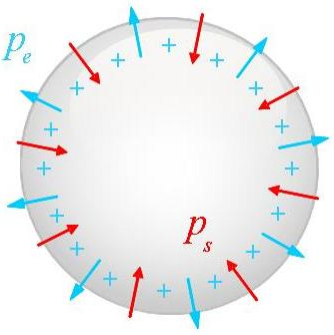

Fig. 2 Theoretical charge distribution of a resting droplet

In a practical external electric field, however, the surface charge on a droplet is generally not uniformly distributed. Because the electric field between the droplets is strongly non-uniform, surface charges tend to migrate toward regions of high curvature, particularly near the droplet tips (Shrimpton 2003). As the inter-droplet distance decreases, both the local electric field and the local surface charge density increase rapidly. The tip region can therefore approach the instability condition earlier than the droplet as a whole. As a result, local Coulomb fission may occur even when the total charge of the droplet is still below the classical Rayleigh limit. This type of breakup can be regarded as a local interfacial instability under sub-Rayleigh-limit conditions (Huo et al. 2012; Shrimpton 2005), triggered by the local accumulation of surface charge.

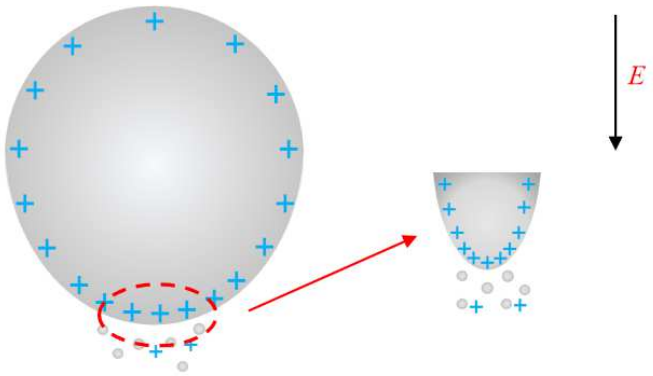

Fig. 3 Charge distribution of a droplet under an applied electric field

For the non-contact interaction of oppositely charged droplets, the strong electric field in the gap not only redistributes surface charge but may also induce gas ionization and space-charge accumulation. The resulting local field distortion further enhances charge accumulation near the droplet tip, allowing one polarity side to reach the instability condition earlier than the other. When the local electric stress exceeds the capillary restoring pressure, the interface becomes unstable and non-contact breakup occurs. Therefore, the non-contact breakup of oppositely charged droplets is closely associated with local electric-field enhancement, surface charge accumulation, and interfacial instability under sub-Rayleigh-limit conditions.

3 Results and Discussion

3.1 Effect of interfacial curvature on breakup polarity

During the approach of two oppositely charged droplets, the upper and lower droplets may have different tip shapes and local interfacial curvatures because of their different supporting conditions. Since the local electric stress is closely related to the interfacial curvature, such geometric differences may affect local charge accumulation and the onset position of interfacial instability. It is therefore necessary to first examine whether the observed breakup polarity is merely a consequence of curvature differences between the two droplets.

To this end, non-contact interaction experiments were performed in air using 20 wt.% NaOH solution droplets and a negative high-voltage power supply. The connection of the negative high-voltage electrode was changed so that either the upper suspended droplet or the lower substrate-supported droplet served as the negative-

polarity droplet. Fig. 4 shows the temporal evolution of the non-contact breakup process under these two electrode configurations. When the negative high voltage was applied to the upper copper wire and the lower hydrophobic substrate was grounded, pronounced Coulomb fission first occurred at the upper suspended droplet, accompanied by the emission of numerous charged daughter droplets. In contrast, the interface of the lower droplet remained relatively stable, and no breakup was observed. When the electrode configuration was reversed, with the lower substrate connected to the negative high voltage and the upper copper wire grounded, the breakup location shifted to the lower droplet. In this case, the lower droplet underwent intense non-contact breakup, whereas the upper droplet remained stable. These observations show that, although the upper and lower droplets differ in supporting condition and local tip curvature, the breakup location always follows the negative-polarity side rather than a fixed geometric position. Therefore, geometric effects associated with droplet size, supporting condition, or interfacial curvature are not the primary cause of the polarity selection. In air, the non-contact breakup of highly conducting oppositely charged droplets exhibits a clear negative-polarity preference, with breakup preferentially initiating from the negative-polarity droplet.

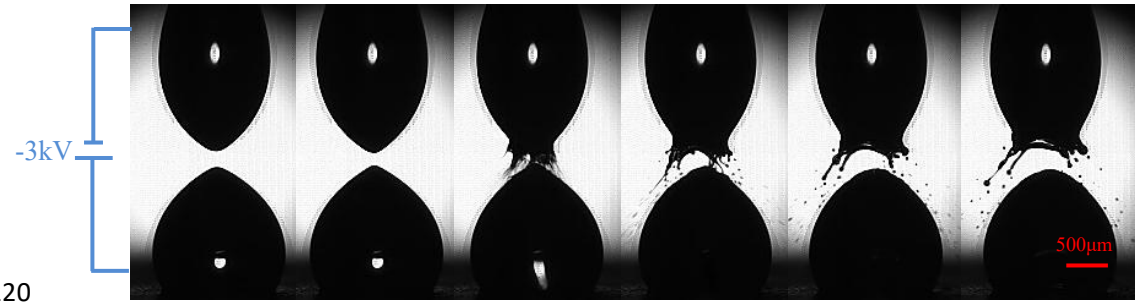

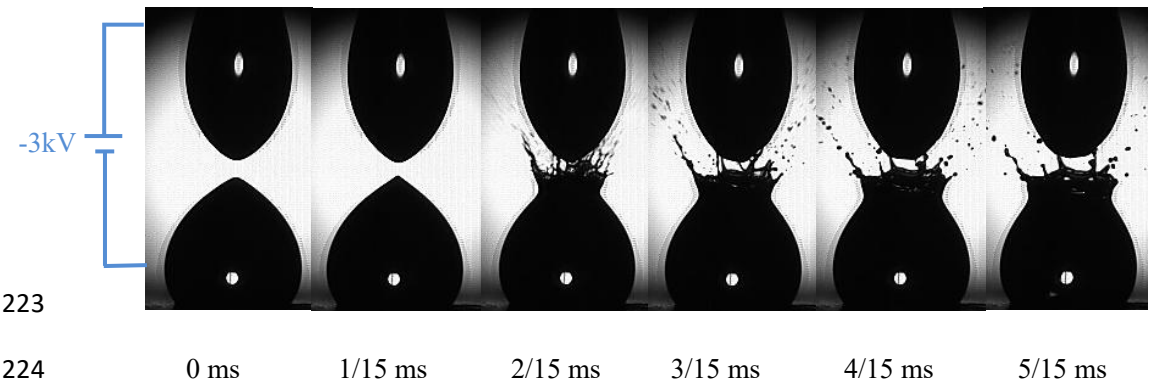

Fig. 4 Temporal evolution of non-contact breakup between oppositely charged droplets in air. (a) The upper droplet was connected to the negative high voltage, and the lower droplet was grounded. (b) The upper droplet was grounded, and the lower droplet was connected to the negative high voltage. The working liquid was a 20 wt.% NaOH solution with an electrical conductivity of 414 μS/cm. The frame rate was 15,000 fps, and the image resolution was 432 × 320 pixels.

3.2 Effect of electrode polarity on breakup polarity

Under a strong electric field, the local electric field is usually enhanced near the high-voltage electrode. It is therefore necessary to determine whether the observed breakup is simply associated with the position of the high-voltage electrode. To this end, non-contact interaction experiments were conducted in air using 20 wt.% NaOH solution droplets and a positive high-voltage power supply. The positions of the positive high-voltage electrode and the grounded electrode were interchanged, so that the upper and lower droplets were alternately placed at the positive high-voltage side and the grounded side.

Fig. 5 shows the temporal evolution of non-contact breakup between oppositely

charged droplets under a positive applied voltage. When the positive high voltage was applied to the upper copper wire and the lower hydrophobic substrate was grounded, breakup did not occur at the upper high-voltage droplet. Instead, interfacial instability first appeared on the lower grounded droplet, which then emitted numerous charged daughter droplets. The upper droplet remained relatively stable, and no obvious breakup was observed. When the electrode configuration was reversed, with the lower substrate connected to the positive high voltage and the upper copper wire grounded, the breakup location shifted to the upper droplet. In this case, pronounced Coulomb fission occurred at the upper droplet, whereas the lower positive high-voltage droplet remained stable. These observations demonstrate that the non-contact breakup of oppositely charged droplets is not determined simply by the position of the high-voltage electrode. Even when a positive high-voltage power supply is used, breakup still preferentially occurs on the relatively negative-polarity side rather than on the positive high-voltage side. Thus, changing the polarity of the applied voltage does not alter the polarity-selection rule. Together with the negative-voltage experiments described in the previous section, these results confirm that, in air, the non-contact breakup of highly conducting oppositely charged droplets exhibits a robust negative-polarity preference.

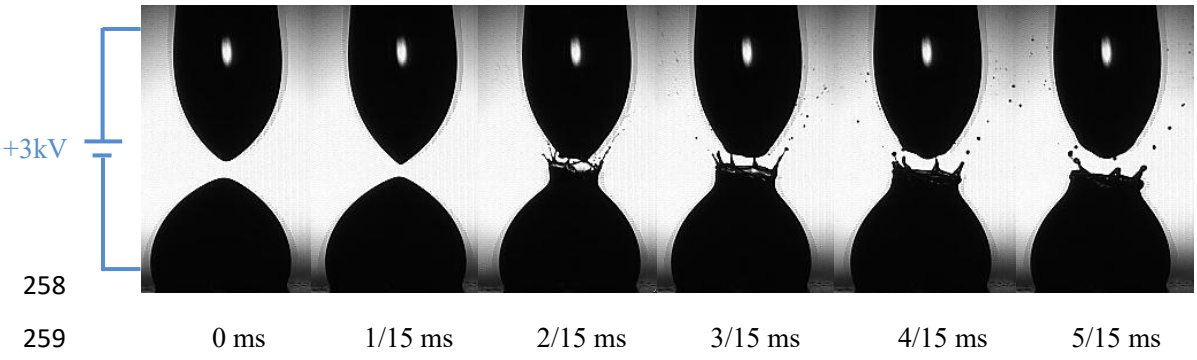

(a)

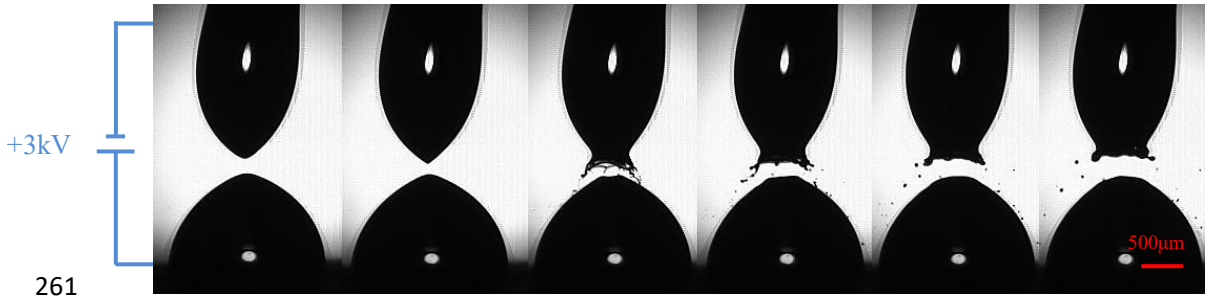

(b)

Fig. 5 Temporal evolution of non-contact breakup between oppositely charged droplets in air under a positive applied voltage. (a) The upper droplet was connected to the positive high voltage, and the lower droplet was grounded. (b) The upper droplet was grounded, and the lower droplet was connected to the positive high voltage. The working liquid was a 20 wt.% NaOH solution with an electrical conductivity of 414 μS/cm. The frame rate was 15,000 fps, and the image resolution was 432 × 320 pixels.

3.3 Effect of pH on breakup polarity

The results in the previous two sections show that the non-contact breakup of oppositely charged droplets always preferentially occurs on the negative-polarity side, and that this polarity selection is not governed by the droplet interfacial curvature or the electrode configuration. To further examine whether this behavior is related to ion migration inside the liquid, the solution pH and the dominant charge carriers were varied to evaluate the effect of liquid-phase ionic mobility on the breakup polarity. A 20 wt.% HCl solution was used as an acidic working liquid, and non-contact interaction experiments were performed in air using a negative high-voltage power supply. Fig. 6 shows the interfacial evolution of HCl solution droplets under two electrode configurations. When the lower droplet was connected to the negative high voltage and

the upper droplet was grounded, non-contact breakup first occurred at the lower negative-polarity droplet. When the upper droplet was connected to the negative high voltage and the lower droplet was grounded, the breakup location shifted to the upper droplet. Thus, although the working liquid was changed from an alkaline NaOH solution to an acidic HCl solution, breakup still consistently occurred on the negative-polarity side.

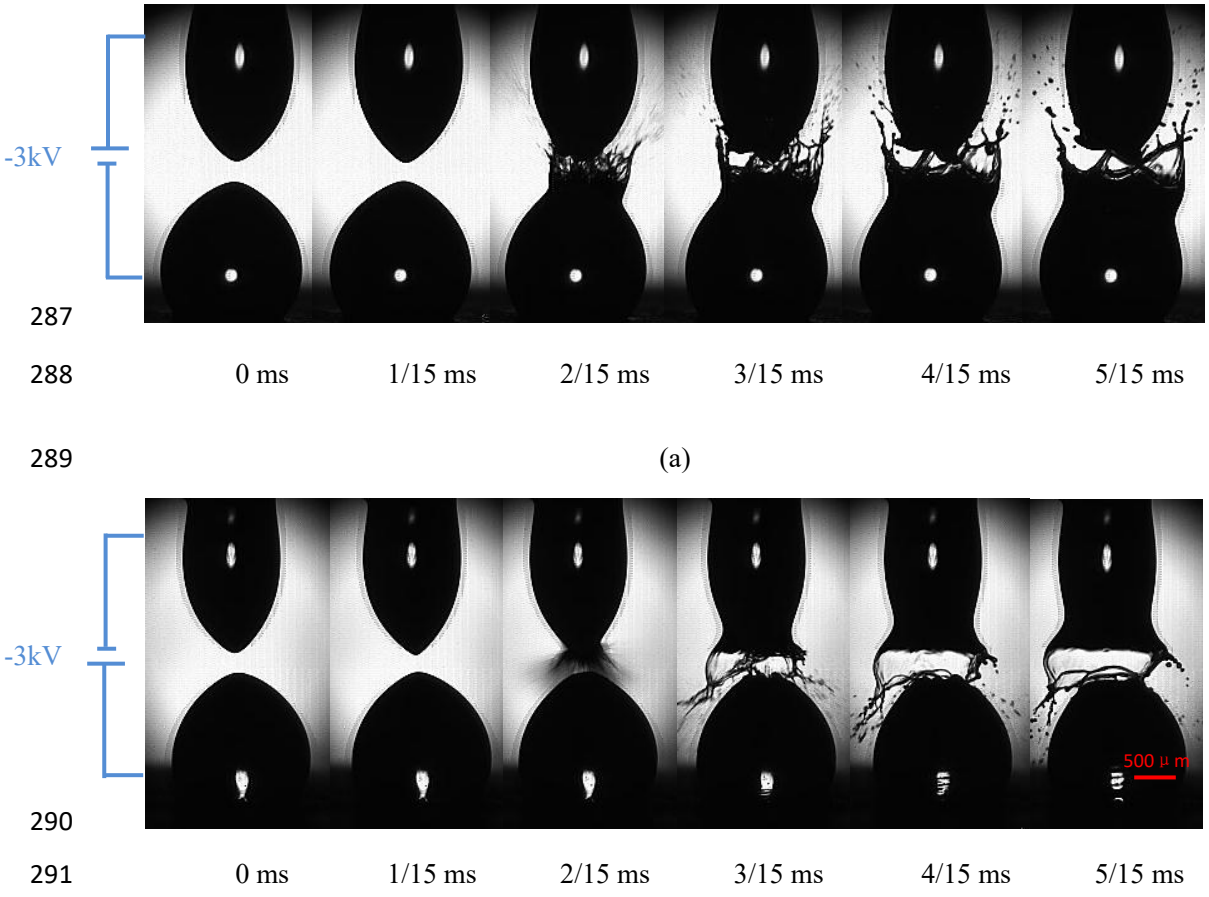

Fig. 6 Temporal evolution of non-contact breakup between oppositely charged HCl solution droplets in air. (a) The upper droplet was grounded, and the lower droplet was connected to the negative high voltage. (b) The upper droplet was connected to the negative high voltage, and the lower droplet was grounded. The working liquid was a 20 wt.% HCl solution with an electrical conductivity of

820 μS/cm. The frame rate was 15,000 fps, and the image resolution was 432 × 320 pixels.

This result can be further examined by considering the mobilities of the major ions in the solutions. Table 2 lists the mobilities of several common ions (Yang et al. 2013). In NaOH solution, the mobility of OH^- is much higher than that of Na^+. If the breakup polarity were controlled by liquid-phase ionic mobility, the rapid accumulation of negative ions near the tip of the negative droplet could appear to explain the preferential breakup on the negative-polarity side. In HCl solution, however, the mobility of H^+ is much higher than that of Cl^-. Following the same ionic-mobility argument, positive charge would be expected to accumulate more rapidly near the tip of the positive droplet, and the positive-polarity side should become more prone to instability. This expectation is inconsistent with the experimental observations, which show that breakup in HCl solution still occurs on the negative-polarity side rather than on the positive side. The comparison between acidic and alkaline electrolyte solutions therefore indicates that the change in pH and the difference in liquid-phase ionic mobility do not determine the polarity selection of non-contact breakup in oppositely charged droplets. In other words, negative-polarity breakup cannot be explained solely by ion migration inside the droplets. Instead, it is more likely associated with gas ionization, space-charge accumulation, and local electric-field distortion in the surrounding gas phase.

Table 2 Ionic mobilities of selected ions in aqueous solutions

Ion	H^+	Na^+	K^+	Li^+	OH^-	Cl^-	SO_4^{2-}
Ionic mobility u($10^{-8}m^2s^{-1}V^{-1}$)	36.23	5.19	7.62	4.01	20.64	7.91	8.29

3.4 Microscopic mechanism of gas-ionization-regulated non-contact breakup polarity

The preceding experiments show that the non-contact breakup of oppositely charged droplets in air consistently exhibits a negative-polarity preference. By varying the droplet interfacial curvature, the polarity of the high-voltage electrode, and the solution pH, the dominant roles of geometric effects, electrode configuration, and liquid-phase ionic mobility can be excluded. The negative-polarity breakup is therefore more likely associated with gas ionization, space-charge distribution, and the resulting local electric-field distortion in the gas surrounding the droplets.

To further examine the role of the gas medium, non-contact interaction experiments were conducted in standard air and helium. Fig. 7 compares the interfacial evolution of oppositely charged droplets in the two gas environments. In standard air, non-contact breakup still occurs only on the negative-polarity side, while the interface of the positive-polarity droplet remains relatively stable. In helium, however, the instability behavior changes markedly, and non-contact breakup can occur at both the positive- and negative-polarity sides. This contrast indicates that the breakup polarity is not determined solely by the charge state of the droplets, but is closely related to the ionization and charged-particle transport characteristics of the surrounding gas.

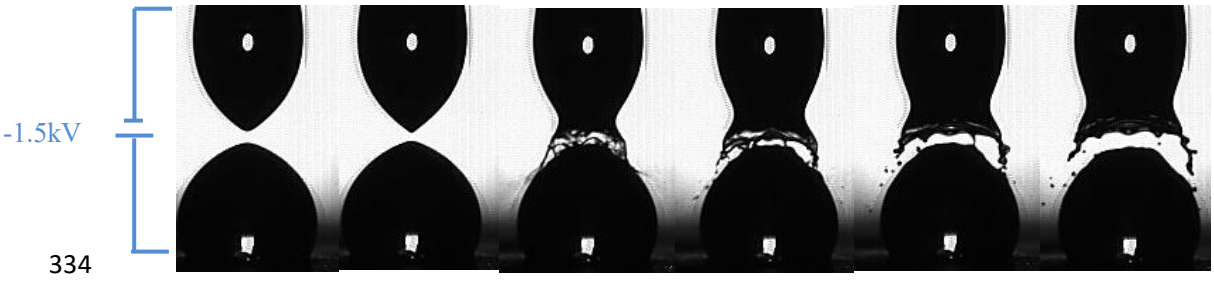

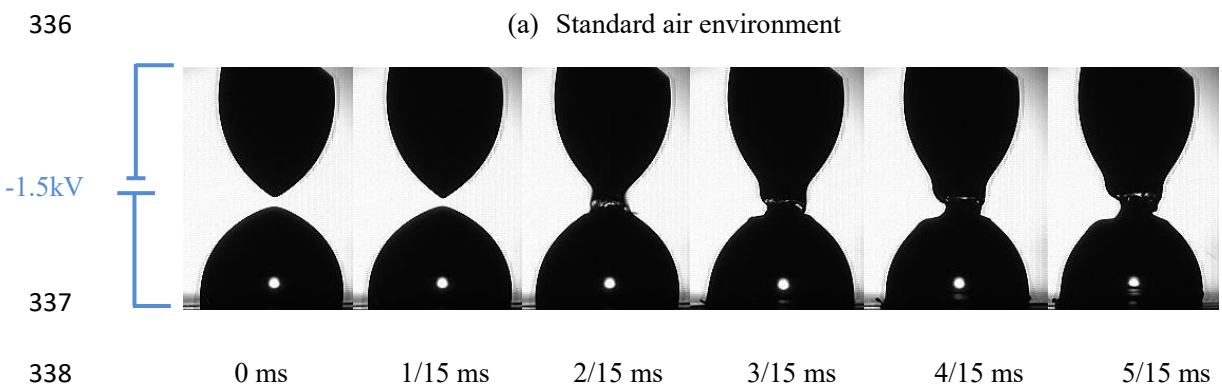

Fig. 7 Temporal evolution of non-contact breakup between oppositely charged droplets in standard air and helium. (a) Standard air environment; (b) helium environment. The working liquid was a 20 wt.% HCl solution with an electrical conductivity of 820 μS/cm. The frame rate was 15,000 fps, and the image resolution was 432 × 320 pixels.

In standard air, when oppositely charged droplets approach each other under a strong electric field, free electrons in the inter-droplet gap are accelerated and trigger impact ionization, leading to the formation of an electron avalanche, as shown in Fig. 8(a). Driven by the electric field, the electrons move toward the positive-potential side and may attach to oxygen molecules in air to form negative ions. At the same time, the heavier and more slowly migrating positive ions, mainly O^{2+} and N^{2+}, drift toward the negative-polarity side and accumulate near the tip of the negatively charged droplet. Since these positive ions cannot rapidly leave the local high-field region, a high-density positive space-charge zone gradually develops near the negative side. This space-charge zone significantly modifies the electric-field distribution in the inter-droplet gap, further enhancing the local electric-field strength and surface charge density at the tip of the negative droplet. Once the local electric stress exceeds the restraining effect of

surface tension, the negative-polarity droplet first reaches a local sub-Rayleigh limit and undergoes Coulomb fission.

In contrast, helium differs markedly from air in terms of ionization and charged-particle transport. As a monatomic inert gas, helium has weak electron attachment and hardly forms stable negative ions. Therefore, the free electrons in the electron avalanche can still migrate rapidly toward the positive-polarity side after leaving the local high-field region. Meanwhile, positive ions in helium, such as He^{2+} and HeH, have relatively high mobility, and their accumulation near the negative-polarity side is weaker than that of positive ions in air, as illustrated in Fig. 8(b). Consequently, the space-charge distribution near the two polarity sides becomes more dispersed in helium, and the local electric-field asymmetry is substantially weakened. The positive-polarity side may also reach the instability condition due to rapid charged-particle transport and local field enhancement, resulting in non-contact breakup at both the positive- and negative-polarity sides.

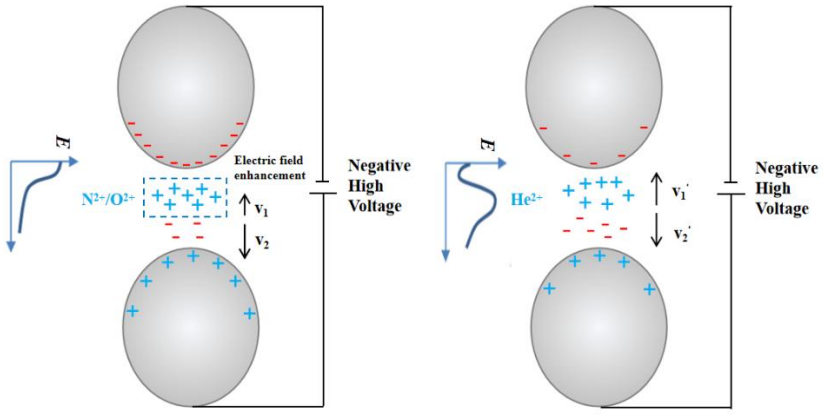

(a) (b)

Fig. 8 Schematic of the space-charge distribution in the inter-droplet gap in standard air and helium. (a) Standard air environment; (b) Helium environment.

To compare the breakup intensity of droplets in air and helium environments, the breakup volume V_b was defined as $V_b = \pi\alpha^2 h/12$, as illustrated in Fig. 9. It represents the volume ejected from the droplet tip during a characteristic time t following the onset of breakup. The onset of breakup was defined as t=0 ms, and the characteristic time was set to 2/15 ms. In the experiments, the breakup volume was determined through image post-processing by measuring the base radius and height of the conical structure formed at the droplet tip. The breakup intensity of the droplet can therefore be quantified by the breakup volume, providing a more direct characterization of the breakup process.

Based on the images in Fig. 7, the breakup volume of the negative-polarity droplet was calculated as V_{air} = 0.61×10-11 m^3 in standard air and V_{He} = 0.29×10-11 m^3 in helium. The larger breakup volume in air indicates that the local electric-field enhancement and surface charge accumulation near the negative-polarity side are stronger in standard air, resulting in more violent breakup. This quantitative comparison is consistent with the proposed mechanism of gas-ionization-induced space-charge accumulation and electric-field distortion, further supporting the role of gas ionization as a microscopic mechanism governing negative-polarity-selective breakup of oppositely charged droplets.

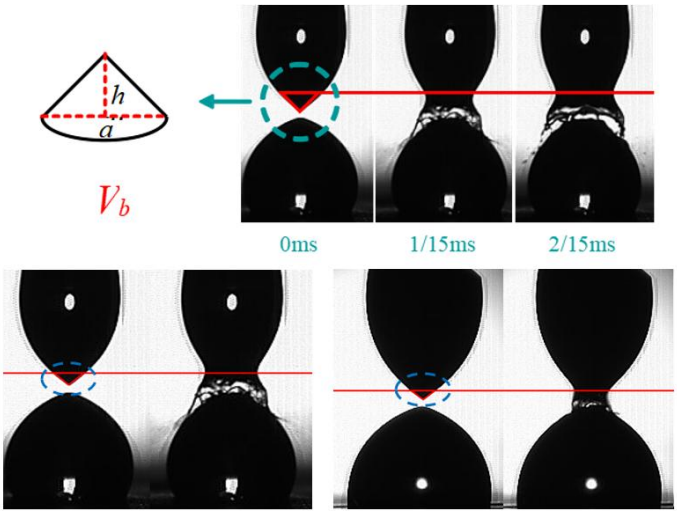

(a) Standard air environment (b) Helium environment

Fig. 9 Measurement of the breakup volume in standard air and helium. (a) Standard air environment; (b) Helium environment.

Furthermore, the critical voltage required for non-contact breakup differs markedly between the two gas environments. Fig. 10 shows the variation in the critical voltage for non-contact breakup of droplets with different electrical conductivities in standard air and helium. In standard air, the critical voltage decreases gradually as the droplet conductivity increases, indicating that higher conductivity facilitates charge transport from the droplet interior toward the interface and tip region. This promotes the formation of a locally high surface charge density and makes the interface more susceptible to Coulomb fission. In helium, the critical voltage for non-contact breakup also decreases with increasing droplet conductivity. However, at the same conductivity, the critical voltage required to trigger non-contact breakup is consistently higher in helium than in standard air. This result indicates that the interfacial dynamics of the droplets are governed not only by charge transport within the liquid phase and interfacial charge accumulation, but also by the ionization characteristics of the

surrounding gas. According to the gas-ionization mechanism discussed above, slow positive ions generated by impact ionization in standard air tend to accumulate near the tip of the negatively charged droplet. This accumulation causes pronounced distortion of the local electric field and further enhances both the electric-field strength and surface charge density at the negative-polarity side. Therefore, at a given applied voltage, the negative-polarity droplet in air may already reach the local sub-Rayleigh limit and undergo non-contact breakup, whereas in helium the weaker electric-field asymmetry between the two polarity sides prevents the droplet interface from reaching the local instability condition required for breakup.

Thus, the comparison of critical voltages provides quantitative support for the physical picture in which gas ionization regulates negative-polarity breakup. By modifying the space-charge distribution and local electric-field strength in the inter-droplet gap, the gas medium affects the accumulation of surface charge at the droplet tip and ultimately determines whether non-contact Coulomb fission preferentially occurs on the negative-polarity side. This result further confirms the key role of gas ionization in the negative-polarity-selective breakup of oppositely charged droplets.

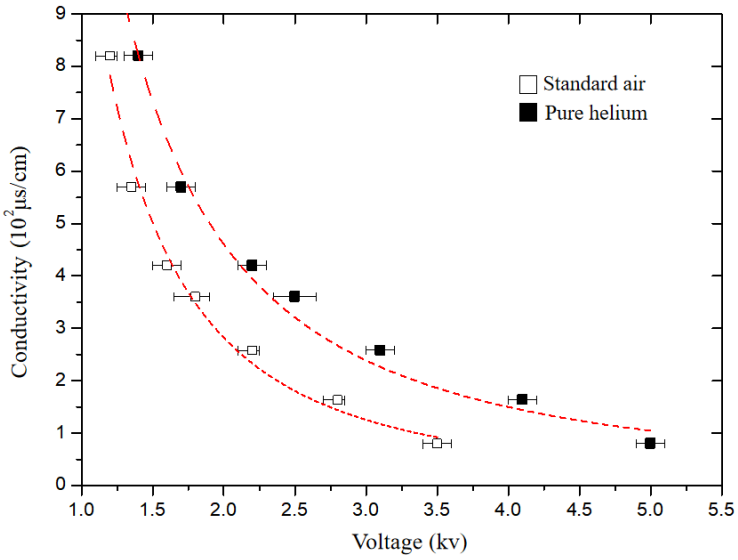

Fig. 10 Critical voltage for non-contact breakup of droplets with different electrical conductivities in standard air and helium.

4 Conclusions

In this study, the non-contact breakup of highly conducting oppositely charged droplets under strong electric fields was investigated in air and helium environments using high-speed microscopic imaging, with emphasis on the polarity selection of breakup and its gas-ionization mechanism. In standard air, non-contact breakup consistently initiated from the negative-polarity side. By varying the interfacial curvature of the upper and lower droplets, reversing the high-voltage-electrode configuration and comparing HCl and NaOH electrolyte solutions, the breakup location was shown to follow the negative-polarity side rather than being governed by droplet geometry, electrode configuration or differences in liquid-phase ionic mobility. Comparative experiments in air and helium further demonstrate that the surrounding gas medium significantly regulates interfacial instability. In air, breakup at the negative-polarity side is more intense, with a larger breakup volume and a lower critical voltage

for non-contact breakup than those in helium at the same droplet conductivity. In helium, by contrast, the reduced electric-field asymmetry between the two polarity sides can lead to non-contact breakup at both sides. These results indicate that, in standard air, slow positive ions generated by impact ionization tend to accumulate near the tip of the negatively charged droplet, forming a local space-charge region that enhances the electric-field strength and surface charge density at the negative-polarity side. As a result, the negative-polarity droplet reaches the local sub-Rayleigh limit first and undergoes Coulomb fission. In helium, weak electron attachment and faster charged-particle transport weaken the local field enhancement near the negative-polarity side. Overall, gas ionization determines the polarity selection and dynamic outcome of non-contact breakup in oppositely charged droplets by regulating the space-charge distribution and local electric-field distortion in the inter-droplet gap. These findings provide useful guidance for interfacial-stability control in electrosprays, microreactors and electric-field-assisted multiphase-flow systems.

Authors' contributions Zhishan Wang： methodology, investigation, formal analysis, visualization and writing of the original draft. Yuanping Huo: conceptualization, supervision, funding acquisition and writing-review and editing. Zhuohang Li, Zirui Wang and Zhentao Wang: investigation, data curation and visualization. Huihe Qiu and Junfeng Wang: supervision, resources and writing-review and editing. All authors read and approved the final manuscript.

Acknowledgements The authors gratefully acknowledge the support of the National

Natural Science Foundation of China.

Funding This work was supported by the National Natural Science Foundation of China (Grant Nos. 52436005, 52076105 and 12102155).

Competing interests The authors declare that they have no competing interests.

Data availability The data supporting the findings of this study are available from the corresponding author upon reasonable request.

Ethics approval and consent to participate Not applicable.

References

Bhalwankar R, Pawar V, Kamra AK (2023) Binary collisions of water drops in presence of horizontal electric fields: a wind tunnel study. Journal of Geophysical Research: Atmospheres 128:e2022JD037543. https://doi.org/10.1029/2022JD037543

Giusti A, Fredrich D (2024) Fuel effects on the electrostatic control of charged droplet trajectories. Fuel 366:131009. https://doi.org/10.1016/j.fuel.2024.131009

Hamlin BS, Creasey JC, Ristenpart WD (2012) Electrically tunable partial coalescence of oppositely charged drops. Physical Review Letters 109:094501. https://doi.org/10.1103/PhysRevLett.109.094501

Huo Y, Zhang C, Zuo Z, et al (2020) Effect of gas ionization on interphase interaction of adjacent oppositely charged droplets. Experiments in Fluids 61:213. https://doi.org/10.1007/s00348-020-03047-w

Huo YP, Wang JF, Mao WL, et al (2012) Measurement and investigation on the deformation and air-assisted breakup of charged droplet. Flow Measurement and Instrumentation 27:92-98. https://doi.org/10.1016/j.flowmeasinst.2012.02.006

Lee MW, Kang DK, Yoon SS, et al (2012) Coalescence of two drops on partially wettable substrates. Langmuir 28:3791-3798. https://doi.org/10.1021/la204867c

Liu T, Seiffert S, Thiele J, et al (2012) Non-coalescence of oppositely charged droplets in pH-sensitive emulsions. Proceedings of the National Academy of Sciences of the United States of America 109:384-389. https://doi.org/10.1073/pnas.1019196109

Liu Y, Huang H, Zhang L, et al (2024) Enhancing the capturing characteristics of charged droplets on submicron particles: an experimental and numerical investigation. Advanced Powder Technology 35:104311. https://doi.org/10.1016/j.apt.2023.104311

Liu Z, Wang P, Li C, et al (2021) Combined effect of charges and external electric field on collision-

coalescence of microns and nanoscale droplets: a numerical simulation perspective. Journal of Molecular Liquids 328:115376. https://doi.org/10.1016/j.molliq.2021.115376

Meng Y, Xia Y, Xu J, et al (2025) Spraying of water microdroplets forms luminescence and causes chemical reactions in surrounding gas. Science Advances 11:eadt8979. https://doi.org/10.1126/sciadv.adt8979

Pawar V, Bhalwankar R, Kamra AK (2024) Effects of eccentricity and horizontal electric field on the characteristics and outcomes of binary collisions of water drops. Geophysical Research Letters 51:e2024GL110547. https://doi.org/10.1029/2024GL110547

Pelesz A, Zylka P (2020) On analytical and experimental aspects of soap bubble stream charging. Experiments in Fluids 61:241. https://doi.org/10.1007/s00348-020-03078-3

Plog J, Jiang Y, Pan Y, et al (2021) Coalescence of sessile droplets driven by electric field in the jetting-based 3D printing framework. Experiments in Fluids 62:56. https://doi.org/10.1007/s00348-021-03153-3

Rayleigh L (1882) XX. On the equilibrium of liquid conducting masses charged with electricity. The London, Edinburgh, and Dublin Philosophical Magazine and Journal of Science 14:184-186. https://doi.org/10.1080/14786448208628425

Ristenpart WD, Bird JC, Belmonte A, et al (2009) Non-coalescence of oppositely charged drops. Nature 461:377-380. https://doi.org/10.1038/nature08294

Shrimpton JS (2003) Pulsed charged sprays: application to DISI engines during early injection. International Journal for Numerical Methods in Engineering 58:513-536. https://doi.org/10.1002/nme.794

Shrimpton JS (2005) Dielectric charged drop break-up at sub-Rayleigh limit conditions. IEEE Transactions on Dielectrics and Electrical Insulation 12:573-578. https://doi.org/10.1109/TDEI.2005.1453462

Sun L, Wang J, Chen Y (2024) Coalescence of multiple droplets induced by a constant DC electric field. PLOS ONE 19:e0300925. https://doi.org/10.1371/journal.pone.0300925

Taylor GI (1964) Disintegration of water drops in an electric field. Proceedings of the Royal Society of London. Series A. Mathematical and Physical Sciences 280:383-397. https://doi.org/10.1098/rspa.1964.0151

Wang D, Wang J, Yongphet P, et al (2020) Experimental study on electric-field-induced droplet generation and breakup in an immiscible medium. Experiments in Fluids 61:78. https://doi.org/10.1007/s00348-020-2908-x

Wang J, Wang B, Qiu H (2014) Coalescence and breakup of oppositely charged droplets. Scientific Reports 4:7123. https://doi.org/10.1038/srep07123

Xu H, Wang J, Wang Z, et al (2025) Review of electrospray cooling and charged droplets heat transfer. Physics of Fluids 37:111303. https://doi.org/10.1063/5.0299519

Yang J, Li Y, Liu R (2013) Theoretical analysis of chloride ion migration tests in cementitious material research. Materials Research Innovations 17:220-223. https://doi.org/10.1179/1432891713Z.000000000219

Zhou Y, Wu J, Gao G, et al (2024) Universal droplet propulsion by dynamic surface-charge wetting. Microsystems & Nanoengineering 10:134. https://doi.org/10.1038/s41378-024-00745-x